Using WISE cataloged data for morphology, bulge fraction and black hole mass estimation

J. Hernández-Yévenes [1]   N. Nagar [1]   V. Arratia [1]   T. H. Jarrett [2, 3]

[1]Departamento de Astronomía, Universidad de Concepción, Chile
[2]Department of Astronomy, University of Cape Town, South Africa
[3]Centre for Astrophysics and Supercomputing, Swinburne University of Technology, Australia

Background

Supermassive black holes (SMBH), ranging from 10^5 to $10^{10} M_\odot$, are present in galactic nuclei [e.g. 4], influencing the evolution and structure of host galaxies [e.g. 13]. SMBHs are commonly found in galaxies with bulges [e.g. 5, 20].

SMBH can appear as Active Galactic Nuclei (AGN), including Quasars (QSO) with luminosities from 10^{44} to 10^{48} erg s^{-1} [12]. QSOs, crucial for probing the early universe, provide insights into galaxy and SMBH formation [24, 8].

The Wide-field Infrared Survey Explorer [WISE, 25] has surveyed the sky in four IR bands (3.4 μm, 4.6 μm, 12 μm, and 22 μm. W1 to W4, respectively). WISE fluxes and colors allow discrimination between different extragalactic objects, estimation of galaxy morphology ($T_{\rm Type}$), and exploration of properties such as total stellar mass (M_*) through photometry [9, 1, 10].

We have developed WISE2MBH [6], an algorithm that takes advantage of WISE data relationships to classify regular galaxies and QSOs, estimate $T_{\rm Type}$, determine bulge-to-total (B/T) mass ratios, and estimate the SMBH mass ($M_{\rm BH}$). The latter are relevant for individual source studies using advanced instruments such as the EHT and ngEHT [19, 11, 2].
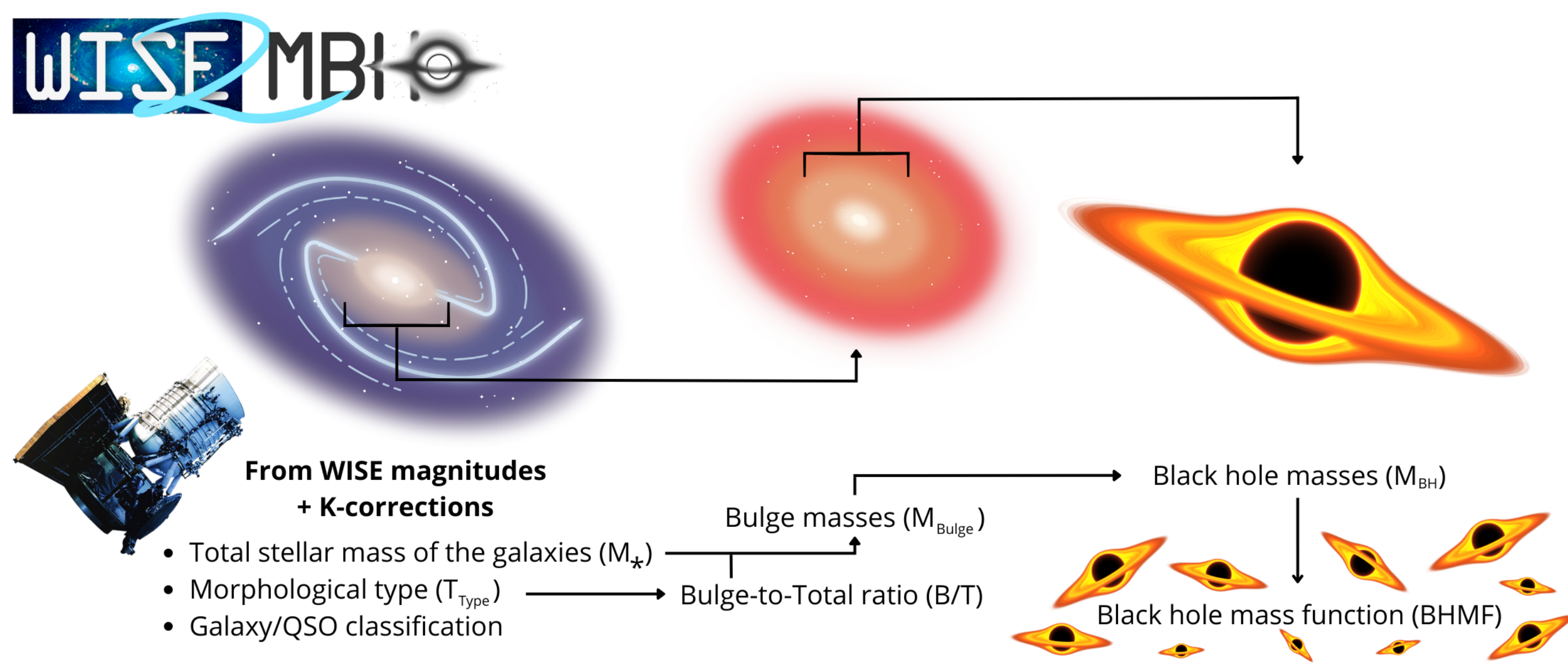

Figure 1. Schematic graph of how WISE data is used to obtain $M_{\rm BH}$ estimates using the WISE2MBH algorithm.

Method: the WISE2MBH algorithm

As shown in Fig. 1, WISE magnitudes (and colors) together with K-corrections up to $z = 3$ from [10] can be used to classify objects into regular galaxies and luminous QSOs using color-color criteria and to obtain properties such as M_* using the method from [1] and $T_{\rm Type}$ using one of our functional fits.

We exploit the empirical evolution of B/T with $T_{\rm Type}$ [e.g. 17, 18] to estimate the former. By combining B/T with M_*, the bulge mass of the galaxy ($M_{\rm Bulge}$) can be obtained.

Both M_* and $M_{\rm Bulge}$ were compared to multiple samples of independently calculated values [e.g. 14]. At lower redshifts, there is good agreement, but as the redshift increases, the differences become more pronounced, as shown in Fig. 2.

Finally, $M_{\rm BH}$ is estimated using the $M_{\rm BH}-M_{\rm Bulge}$ scaling relation from [21]. An empirical compensation factor (C_f) is calculated using measured and highly reliable estimates of $M_{\rm BH}$ and then applied to the obtained estimate.

The WISE2MBH algorithm implements a Monte-Carlo approach for error propagation, considering WISE photometric errors and uncertainties in the conversion factors used. Errors in scaling relations are convolved with this distribution, if available, as in the case of [21]. From the final distribution, both the median value and 1σ errors are saved.

This algorithm is applied to the Event Horizon and Environs sample [ETHER, 19], which compiles more than 3 million extragalactic sources with spectroscopic redshifts. With such a huge sample, the local black hole mass function (BHMF) can be calculated using $M_{\rm BH}$ estimated from our algorithm, which gives us insight on the populations of SMBH in the local Universe.
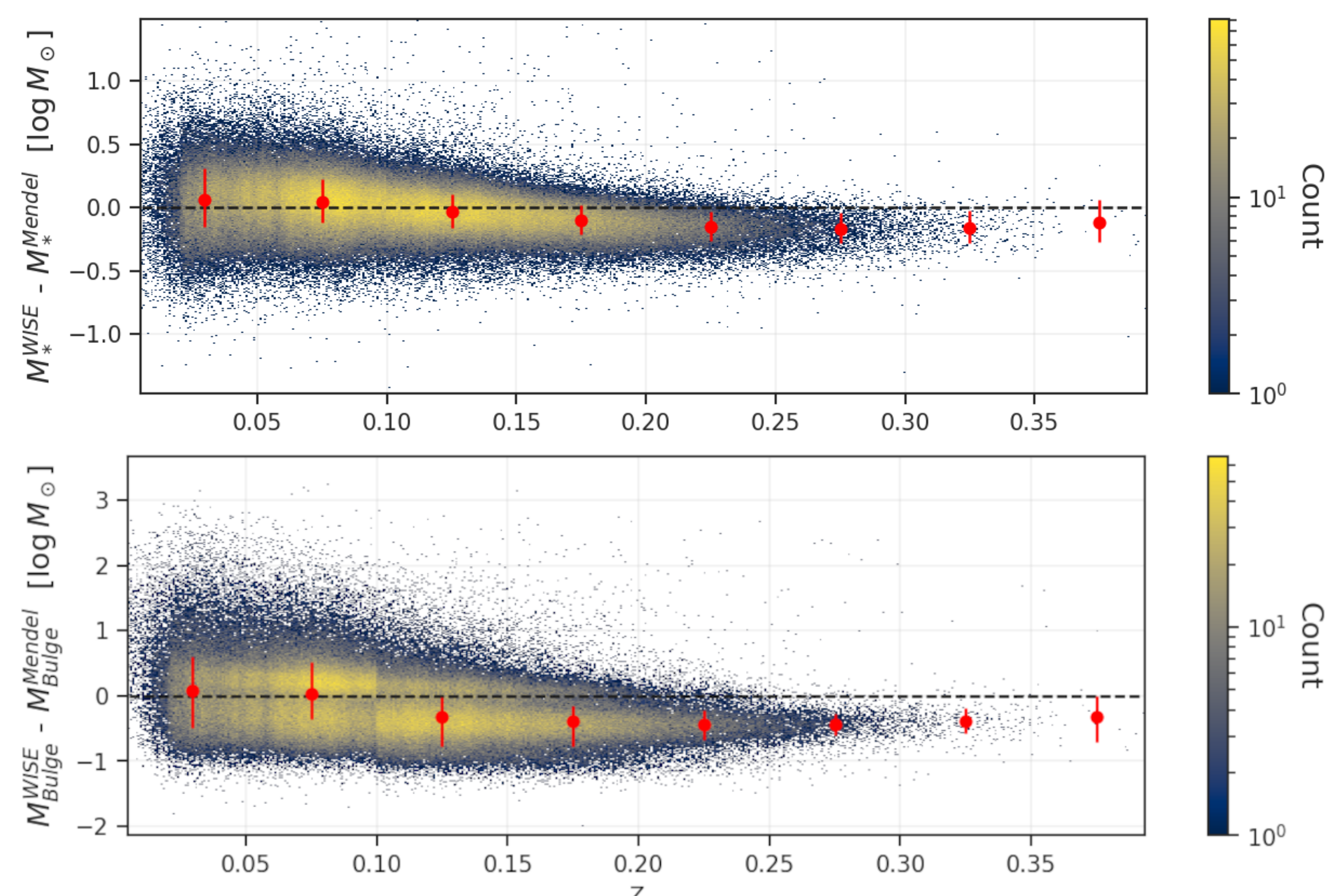

Figure 2. Difference between WISE-derived M_* (**Top**) and $M_{\rm Bulge}$ (**Bottom**) and the low redshift ($z \leq 0.4$) sample of [14] against redshift. The black dashed line shows the line of equality and red dots with error bars represent the median and 1σ dispersion of the difference between masses for slices of 0.05 in redshift. Colors represent the density of objects following the color bar to the right.

Color-color criteria and functional fits

For QSO selection, we combine a slightly modified version of the boxy region described by [9] and a line division at W1−W2= 0.8 [e.g. 23]:

$$W2-W3 < 2.2 \wedge W1-W2 > 0.8$$
$$2.2 < W2-W3 < 4.4 \wedge W1-W2 > (0.05[W2-W3] + 0.38)$$

Every source that does not meet this criteria is considered a regular galaxy, and every source with a color W2−W3> 4.4 is rejected due to uncertain classification.

In our work, we compared manually obtained $T_{\rm Types}$ from the 2MRS sample [7] to WISE W2−W3 colors. Their relationship can be described by an S-shape curve with the following functional fit:

$$W2-W3_{\rm SN} = (W2-W3 - 0.75)\,/2.71$$

$$T_{\rm Type} = (1.21 \pm 0.01)\, {\rm logit}\,(W2-W3_{\rm SN}) + (1.36 \pm 0.02)$$

Using multiple independently derived B/T from the literature [e.g. 14, 15], we found an exponentially decreasing trend with $T_{\rm Type}$ that is described with the following functional fit:

$$B/T = 0.05 + 0.36 \left(7.72^{-0.1 \cdot T_{\rm Type}}\right)$$

The obtained C_f is calculated using the estimated $M_{\rm BH}$ and then adding it to the latter:

$$C_f = -0.18 \log M_{\rm BH} + 1.73$$

Despite their simplicity, functional fits yield results that are generally in good agreement with observational and theoretical predictions of SMBH masses, both in individual cases and populations.

Results

Applying the WISE2MBH algorithm to a crossmatch of ETHER and AllWISE with sources with $z \leq 3$, the algorithm provides ~2.6 million $M_{\rm BH}$ estimates (68% new) and ~730 thousand upper limits, with almost 80% of the final sample being first-time $M_{\rm BH}$ estimates or upper limits.

When comparing the same subset of measured and highly reliable estimates of $M_{\rm BH}$ used to derive C_f with their WISE2MBH counterparts, a Spearman score of ~0.8, R^2 of ~0.68 and RMSE of ~0.52 were obtained, showing a great correlation and no large scatter (see Fig. 3). The uncertainties in the estimated $M_{\rm BH}$ (in log $M_\odot$) were shown to be around ±0.5 at all possible values of B/T, few with uncertainties as high as ±1.2 in the low bulge-fraction regime (LBF, $B/T < 0.3$). The most relevant sources appear at high bulge-fraction (HBF, $B/T > 0.4$), where first-time estimates for elliptical galaxies are being used for source selection in multiple observational proposals.

The black hole mass function (BHMF) of the WISE2MBH final sample is in good agreement with other previously and independently derived BHMFs. The ETHER sample has few low mass estimates (log $M_{\rm BH} \leq 6$), while the WISE2MBH final sample can provide this population of sources, and the overall combination of both samples generates the most complete BHMF (see Fig. 3).
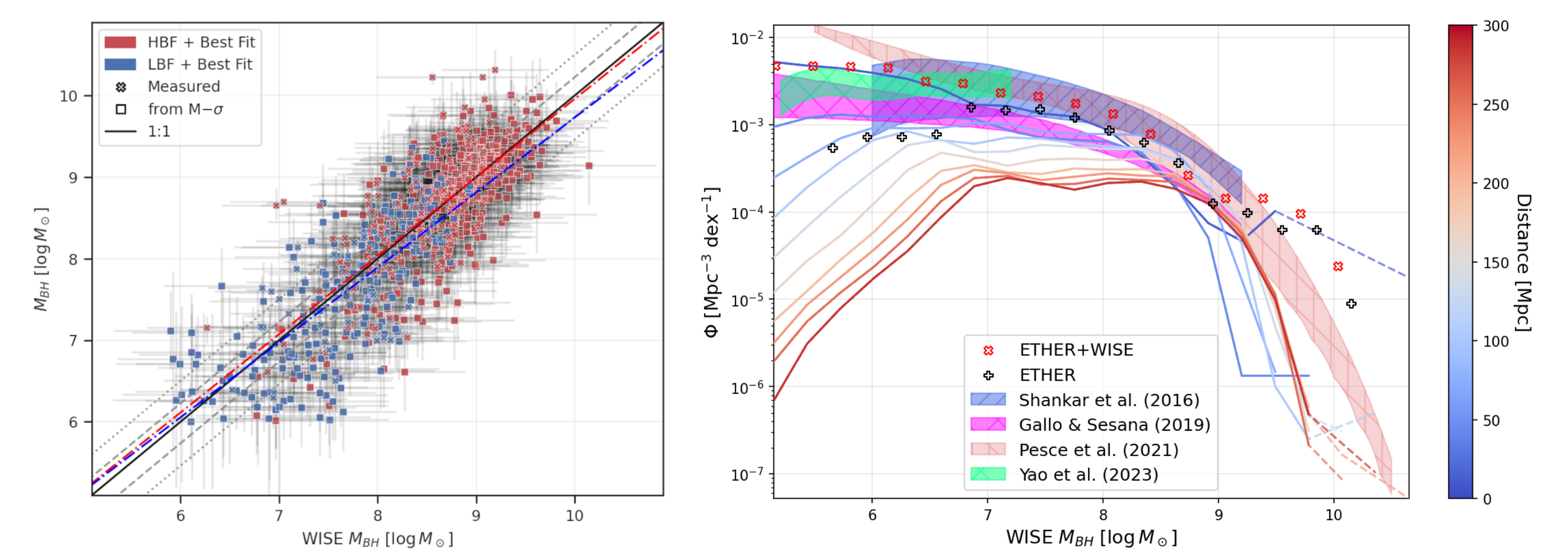

Figure 3. **Left:** A comparison of measured (cross) and highly reliable estimated (box) black hole masses against WISE-derived $M_{\rm BH}$ values in the WISE2MBH final sample. Data points include 1σ error bars. High bulge-fraction (HBF) and low bulge-fraction (LBF) galaxy subsamples and their best fit linear regressions are color-coded, along with 1σ prediction intervals (dashed lines) and RMSE scatter (dotted lines), are shown. **Right:** BHMF in the WISE2MBH final sample for 30 Mpc-wide shells at distances from 30 to 300 Mpc, indicated by the color bar. ETHER+WISE and ETHER points represent the BHMF from ETHER, with and without WISE $M_{\rm BH}$ estimates. Reference literature BHMFs from [22], [3], [16], and [26] are shown for comparison.

Summary

The WISE2MBH algorithm is available on **GitHub** and classifies galaxies and QSOs using WISE catalog data. It estimates stellar masses (M_*), morphological types ($T_{\rm Type}$), bulge-to-total ratios (B/T), and black hole masses ($M_{\rm BH}$) or upper limits. Applying scaling relations, it derives $M_{\rm BH}$ from a parent sample of ~ 3.8 million sources, producing ~ 2.6 million $M_{\rm BH}$ estimates and ~ 730 thousand upper limits. This algorithm, incorporated into the ETHER sample, is helpful for EHT and ngEHT studies, offering new source samples as candidates for observation with these facilities.

References

[1] Cluver M. E., et al., 2014, ApJ, 782, 90
[2] Doeleman S. S., et al., 2023, Galaxies, 11, 107
[3] Gallo E., Sesana A., 2019, ApJL, 883, L18
[4] Graham A. W., 2016, Galaxy Bulges and Their Massive Black Holes: A Review. Springer International Publishing, Cham, pp 263–313
[5] Gültekin K., King A. L., Cackett E. M., Nyland K., Miller J. M., Di Matteo T., Markoff S., Rupen M. P., 2019, ApJ, 871, 80
[6] Hernández-Yévenes J., Nagar N., Arratia V., Jarrett T. H., 2024, Submitted to MNRAS
[7] Huchra J. P., et al., 2012, ApJS, 199, 26
[8] Inayoshi K., Visbal E., Haiman Z., 2020, ARA&A, 58, 27
[9] Jarrett T. H., et al., 2011, ApJ, 735, 112
[10] Jarrett T. H., Cluver M. E., Taylor E. N., Bellstedt S., Robotham A. S. G., Yao H. F. M., 2023, ApJ, 946, 95
[11] Johnson M. D., et al., 2023, Galaxies, 11
[12] Kong M., Ho L. C., 2018, ApJ, 859, 116
[13] Kormendy J., Ho L. C., 2013, ARA&A, 51, 511
[14] Mendel J. T., Simard L., Palmer M., Ellison S. L., Patton D. R., 2014, ApJS, 210, 3
[15] Morell D. F., Ribeiro A. L. B., de Carvalho R. R., Rembold S. B., Lopes P. A. A., Costa A. P., 2020, MNRAS, 494, 3317
[16] Pesce D. W., et al., 2021, ApJ, 923, 260
[17] Quilley L., de Lapparent V., 2022, A&A, 666, A170
[18] Quilley L., de Lapparent V., 2023, arXiv e-prints, p. arXiv:2305.02069
[19] Ramakrishnan V., et al., 2023, Galaxies, 11
[20] Saglia R. P., et al., 2016, ApJ, 818, 47
[21] Schutte Z., Reines A. E., Greene J. E., 2019, ApJ, 887, 245
[22] Shankar F., et al., 2016, MNRAS, 460, 3119
[23] Stern D., et al., 2012, ApJ, 753, 30
[24] Wang F., et al., 2021, ApJL, 907, L1
[25] Wright E. L., et al., 2010, AJ, 140, 1868
[26] Yao Y., et al., 2023, ApJL, 955, L6